X-Ray Photoelectron Spectroscopy Study of NaH₂PO₄/CeP₂O₇ Powder Electrolyte

Pushpanjali Singh

Department of Physics, Teerthanker Mahaveer University, Moradabad, 244001, Uttar Pradesh, India. E-mail: Singhpushpi111@gmail.com

Amit Kumar Sharma

Department of Physics,
Teerthanker Mahaveer University, Moradabad, 244001, Uttar Pradesh, India.

*Corresponding author: amit.db1980@gmail.com

Pawan Kumar

Department of Physics, Gurukula Kangri University, Haridwar, 249404, Uttarakhand, India. E-mail: pksoniyal13@gmail.com

(Received on October 4, 2024; Revised on November 4, 2024 & December 8, 2024 & January 29, 2025; Accepted on February 10, 2025)

Abstract

This study employs X-ray photoelectron spectroscopy (XPS) to investigate the surface compositions and electronic structure of NaH₂PO₄/CeP₂O₇ powder electrolytes with potential applications in the field of energy storage devices. The samples were synthesized by chemical route method. The result reveals the presence of sodium, cerium, phosphorous and oxygen, with their respective states. The Ce 3d and P 2p spectra indicates the presence of Ce (IV) and PO₄³⁻ species, respectively. The Na 1s and O 1s spectra suggest the presence of sodium phosphate and cerium phyrophosphates phases. The obtained results also explore the physical and chemical properties of prepared electrolytes such as oxidation states, elemental analysis and binding energy of prepared electrolytes. This study provides a detailed understanding of surface mechanism of NaH₂PO₄/CeP₂O₇ electrolytes. This work also gives a complete explanation of the surface mechanism and the existence of NaH₂PO₄/CeP₂O₇ elements in powder electrolytes, as well as identifies the chemical states based on the observed peak and binding energy, verifying the presence of elements in the samples.

Keywords- XPS, Sodium dihydrogen phosphate, Cerium pyrophosphate, Elemental analysis, Binding energy.

1. Introduction

Low-emission and high-efficiency fuel cells are traditional energy source to convert chemical energy into electrical energy directly. The solid acid electrolytes are good potential materials for sensors, memory cells, fuel cells and solid-state batteries, they have high-quality mechanical properties (Owens, 2000). Potential of NaH₂PO₄ (SDP) in the future generation of sodium ion batteries is recently explored (Singh et al., 2024a). Structural features of this material are considered to have inductive impact of phosphate-based functional groups to boost their working capacity (Zhang et al., 2021). At low temperatures, SDP is a significant material due to its high stability of sodium ions (Martsinkevich and Ponomareva, 2012). Because of good stability of sodium ions (Zhang et al., 2015; Rhimi et al., 2018), this material also finds applications in water treatment, food, chemical refineries medical, and other areas (Kumar et al., 2024, Zhang et al., 2014; Rybalkina et al., 2019). It is also used as a fuel and detergent element (Chen et al., 2014; Huang et al., 2018).



This material crystallizes in monoclinic symmetry with space group P21/c and a tunnel structure (Zhang et al., 2015; Rhimi et al., 2018). It has many properties including good ionic conductivity. Properties of this material is influenced by the doping (Yoshimi et al., 2008; Cheng et al., 2021). When cerium pyrophosphates are mixed with a solid acid, they create strong surface interactions that immobilize the solid acid (Jain et al., 2018). Thus, surface elemental analysis of synthesized materials may throw light on such mechanism. X-ray photoelectron spectroscopy (XPS) is widely used for measuring the density of electronic states of the metallic catalyst and the chemical composition of material surfaces within the range of 10 nm. Generally, the detection sensitivity is nearly 0.1–1.0 atomic % for all elements except H and He, making it a unique technique for surface characterization (Lubenchenko et al., 2018). The surface charges in insulating samples can cause XPS peak shifts, broadening and asymmetries, leading to false results (Barker et al., 2005; Kloprogge and Wood, 2016; Lubenchenko et al., 2018; Greczynski and Hultman, 2020; Veer et al., 2022), hence, the utmost care is needed to perform XPS measurements.

XPS has irradiating a material with X-rays and measuring the (K.E) kinetic energy of photoelectrons emitted from different energy levels of the material's surface atoms using a hemispherical analyzer. A variant of the binding energy (BE) of an electron in a certain energy level of an element (atom) relative to the Fermi level, gives a chemical shift that occurs in the oxidized state or in the distribution of electrical charges around the nucleus changes due to change in chemical bonds of the element in the environment (Stevie and Donley, 2020). Considering the importance of XPS analysis, this study is focused on the elemental analysis surface mechanism in NaH_2PO_4/CeP_2O_7 powder electrolytes.

2. Materials and Methods

SDP powder was prepared by mixing Na₂CO₃ (Alfa-Aesar, 99.9%) and aqueous phosphoric acid H₃PO₄ (Alfa-Aesar 85%) in deionized water at a molar ratio.

$$Na_2CO_3 + 2H_3PO_4 \rightarrow 2NaH_2PO_4 + CO_2 + H_2O$$
.

The resulting slurry was found to be hardened when placed in an oven. Methanol was used to precipitate the solid layer and then filtered. SDP was sintered at 120 °C for 12 hours to remove residual water and then ground into a fine powder. CeO₂ (25 g) and H₃PO₄ (23 mL) were mixed in a crucible and heated at 300 °C for 6 h to form a CeP₂O₇ matrix. The sample was dried at 140 °C for 24 h, then milled and was kept at a temperature of 110 °C for another 12 h. The sample was calcined at 550 °C for 6 h and are analysed by X- ray diffraction to check phase transition of CeP₂O₇. Furthermore, it was combined with SDP in different molecular weight ratios (Singh et al., 2024b).

Finally, the four samples like S1(0.9SDP/0.1CeP₂O₇), S2(0.8SDP/0.2CeP₂O₇), S3(0.7SDP/0.3CeP₂O₇), and S4 (0.6SDP/0.4CeP₂O₇) were prepared using a mechanical grinding process. To produce fine structure of solid acid composite powders, all samples were kept in an oven at 120 °C temperature for 1 h (Singh et al., 2024b). An XPS measurement typically has a depth of analysis of about 5 nm. The fine solid acid composite powder was pressed onto contamination-free adhesive tape, like double-sided sticky carbon tape, to create a pellet for the powder samples used in XPS analysis as shown in **Figure 1**. Then it is applied to examine the prepared composites. The analyzer's work function is 4.478 eV. The energy source the pass energy is used at 376 eV to allow electrons to entre at the detector slits.

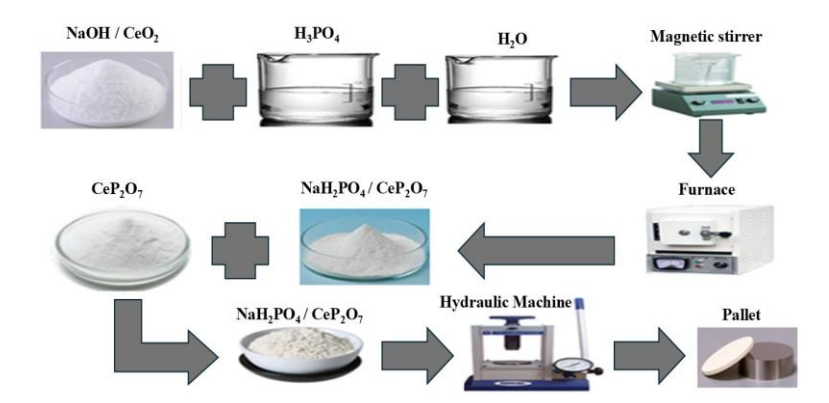


Figure 1. Chemical route method to synthesise SDP and CeP₂O₇, and the preparation of their composites.

3. Results and Discussion

XPS analysis was performed to elucidate the chemical state of the elements for S1, S2, S3, S4 and pure SDP. The spectra of the survey scans (**Figure 2**) revealed presence of O, Na and P atoms in pure SDP nanocomposite, while O, C, P, Na, Ce in S1, S2, S3 and S4 can be seen in **Figure 2**.

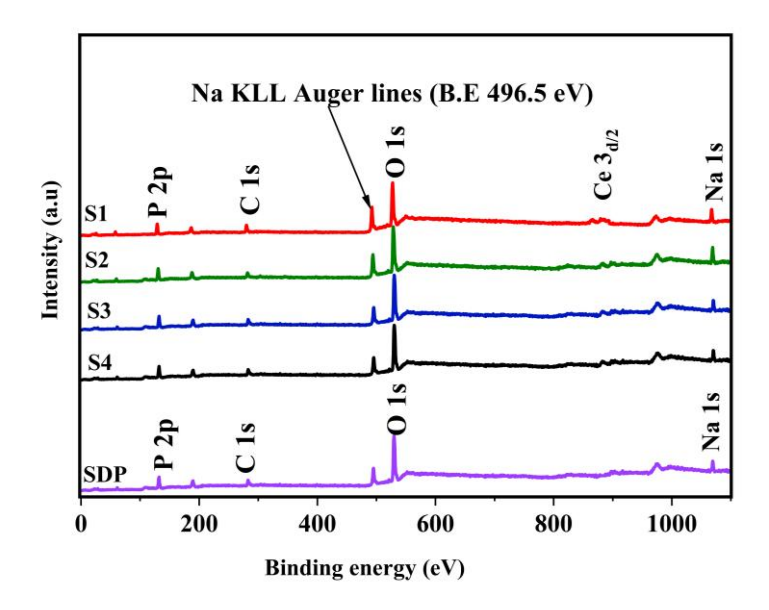


Figure 2. XPS survey spectra of S1, S2, S3, S4 and SDP samples.

The XPS wide scan spectra for different elements of sample S1 are analyzed to obtain specific information on the oxidation state and surface chemical species. The P(2p) binding energy usually ranges between 129 and 136 eV, depending on the phosphorus's chemical environment. It depends upon the bonding environment and the level of oxidation. The oxidation state of phosphorus can be ascertained by examining the binding energy (BE) shifts in the P(2p) spectrum in XPS (Mallet et al., 2013; Zhang et al.,

2021). The P(2p) peak location is shifted and the electron density surrounding the phosphorus atom is altered by the various oxidation states, which correlate to distinct chemical environments. Higher oxidation states cause phosphorus and oxygen to be more attracted to one another, which withdraws electron density and raises binding energies.

In **Figure 3**, the P(2p) spectrum can be observed at binding energies of 132.5 eV and 132.1 eV (Mallet et al., 2013; Zhang et al., 2021), respectively. The P(2p) peak in NaH₂PO₄·2H₂O had a binding energy (BE) of 132.5 eV, which was much lower than that of phosphate adsorption (133.6 eV), according to Moulder et al. (1992), Mallet et al. (2013), Yao et al. (2021), Spin-orbit coupling causes the P (2p) peak splitting into two components, with the higher intensity P $2p_{3/2}$ peak (134.6 eV) always being more intense than the lower intensity P $2p_{1/2}$ (Spin-orbit split component, 133.9 eV).

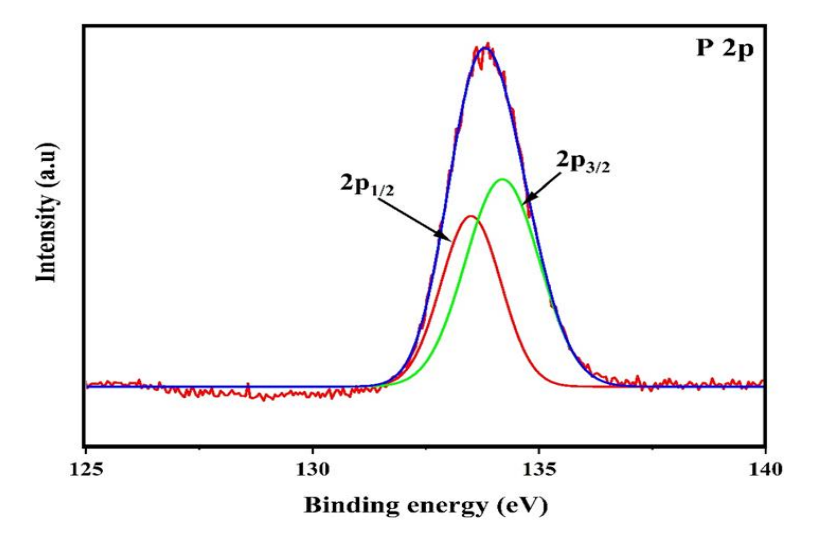


Figure 3. De-convoluted P (2p) wide scan spectrum of sample S1.

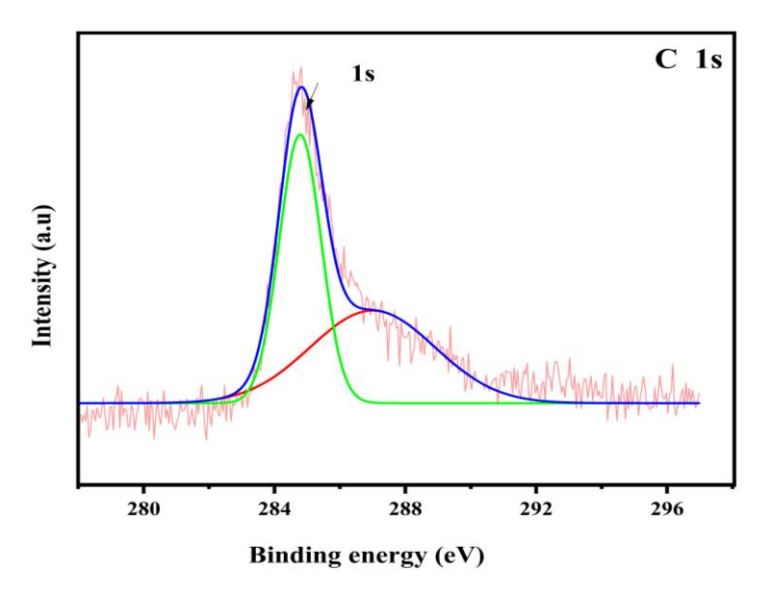


Figure 4. De-convoluted C 1s wide scan spectrum of sample S1.

Furthermore, C1s spectrum of this material is shown in **Figure 4**, which exhibits two de-convoluted peaks at 284.67 eV, and 286.98 eV. Generally, C1s spectra show the separate peaks for various chemical environments of carbon atoms. According to the measured peaks based on the binding energy shifts caused by various chemical bonding states, sp² hybridized carbon with metal contacts are indicated by 284.11 eV, where the electron density is pushed towards the metal, lowering the binding energy. The strong electronegative action of oxygen causes carbon to lose electron density, which raises the binding energy and causes 284.67 eV and 286.98 eV. Because of aliphatic/aromatic hydrocarbons, the deconvoluted C1s spectrum has peaks at binding energies of 284.6–285.0 eV (Siow et al., 2018; Chen et al., 2020; Zhang et al., 2021). As seen in **Figure 4**, the primary signal is detected at 284.3 eV, whereas the secondary signal is found at 288.5 eV as a result of O–C=O.

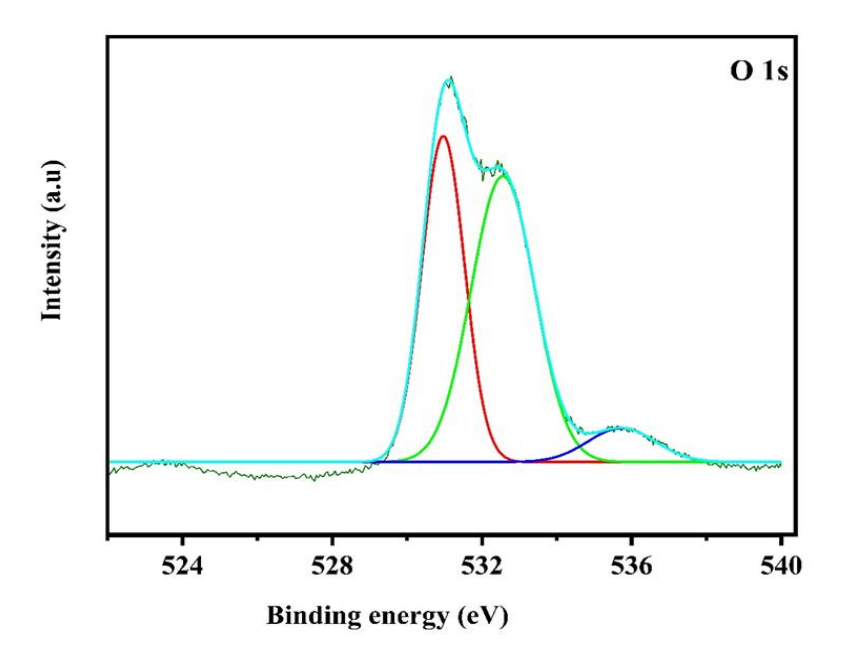


Figure 5. De-convoluted O 1s wide scan spectrum of S1 sample.

Figure 5 indicates the appearance of various types of oxygen species, with two peaks centered at 531.03 eV due to lattice oxygen (O^{2-}) in P_2O_7 and at 533.12 eV due to phosphate oxygen (i.e. PO^- in PO_4^{3-}). The chemisorbed oxygen in the form of M-OH (caused by moisture) over the surface of nanocomposites is responsible for a high binding energy in the O1s peak at 531.03 eV (Teterin et al., 1998; Janos et al., 2017; Zhang et al., 2021; Kumar et al., 2023).

Figure 6 shows the XPS spectrum of the Na Is photoelectron spectra. As can be seen from this figure, the Na peaks are symmetrical with a half-width of \sim 2 eV for S1 sample. Although there is a very small shift to lower binding energy, this suggests that the sodium atoms are in a bonding configuration. As shown in **Figure 7**, the co-existence of oxidation states Ce^{3+} and Ce^{4+} can be distinguished (Uma et al., 2014; Huang et al., 2017; Jian et al., 2020). The XPS spectrum of $Ce^{(3d_{3/2})}$ and $Ce^{(3d_{5/2})}$ obtained from tiny particles. In addition, on the Ce^{3+} doped CeP_2O_7 sample, Ce^{4+} reactive energy peaks at 884.1 eV, 898.5 eV, and two Ce^{3+} species peaks at 881.7 eV and 903.1 eV were clearly visible as summarized in **Table 1**. The spectral structure indicates the presence of two oxidation states, Ce^{4+} and Ce^{3+} are confirming the successful doping of CeP_2O_7 in the samples.

Core level	State	BE(±0.1eV)	Assignment
P 2p _{1/2}	\mathbf{P}^0	132.5	Non-metal
_	\mathbf{P}^{3+}	133.8	Oxide
	P ⁵⁺	140.5	Oxide
C 1s	p^0	284.67	Non-metal
O 1s	O ²⁺	531.23	Non-metal
Na 1s	Na ¹⁺	1071	Metal
Ce 3d _{5/2}	Ce ⁰	884.5	Metal
Ce 3d _{3/2}	Ce ¹⁺	898.5	Oxide

Table 1. Peak centre, peak width and fitting parameters of sample S1 all elements.

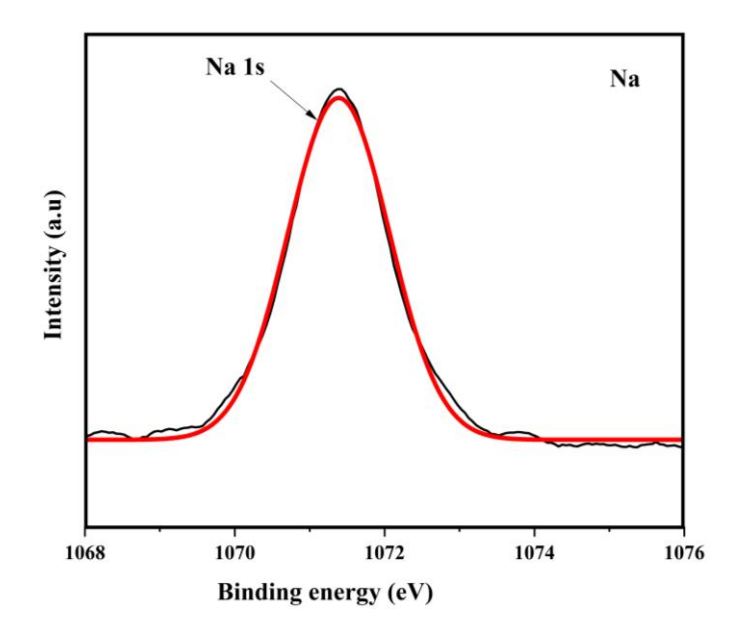


Figure 6. De-convoluted of Na 1s wide scan spectrum of S1 sample.

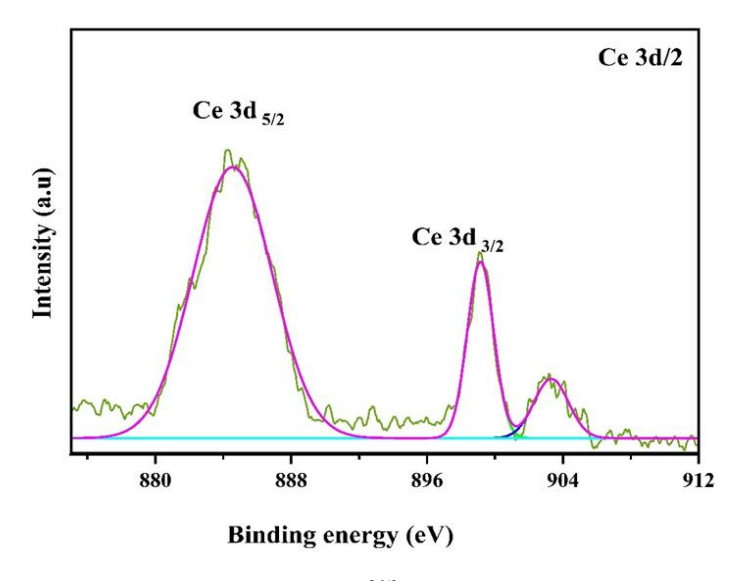


Figure 7. De-convoluted of and Ce^{3d/2} wide scan spectrum of S1 sample.



4. Conclusions

Thus, 0.9 NaH₂PO₄/0.1CeP₂O₇ powder electrolyte was successfully synthesized. Onsets of carbon-metal interactions, phosphate adsorption and presence of hydrocarbons are found as evidenced from the X-ray photoelectron spectroscopy (XPS). Signature of moisture-induced chemisorbed oxygen over the surface of nanocomposites is also observed. Two oxidation states, Ce³⁺ and Ce⁴⁺, are visible in the spectrum structure, confirming that CeP₂O₇ was successfully doped in the samples. Thus, XPS study provides valuable insight into the chemical states of CeP₂O₇ within the material, helping to understand its surface properties and reactivity in S1 sample. The findings on the role of CeP₂O₇ suggest that this can be a possible potential candidate for energy storage devices.

Conflict of Interest

The authors affirm that no known competing financial interests could have influenced any of the work described in this study.

AI Disclosure

The author(s) declare that no assistance is taken from generative AI to write this article.

Acknowledgments

Pushpanjali Singh (TEN22 Ph.D./511) would like to thank Teerthanker Mahaveer University, Moradabad for awarding a PhD scholarship and IIT Roorkee for XPS Characterization.

References

- Barker, J., Gover, R.K.B., Burns, P., Bryan, A., Saidi, M.Y., & Swoyer, J.L. (2005). Structural and electrochemical properties of lithium vanadium fluorophosphate, LiVPO4F. *Journal of Power Sources*, *146*(1-2), 516-520.
- Chen, X.Z., Tang, J.H., Cui, Y.N., Liu, M., & Mao, D. (2014). Phase equilibrium for the ternary system NaH2PO4+ Na2SO4+ H2O in aqueous solution at 298.15 K. *Journal of Chemical & Engineering Data*, 59(2), 481-484.
- Chen, X., Wang, X., & Fang, D. (2020). A review on C1s XPS-spectra for some kinds of carbon materials. *Fullerenes, Nanotubes and Carbon Nanostructures*, 28(12), 1048-1058.
- Cheng, Y., Wei, B., Liu, Y., & Cheng, Y. (2021). Plasma electrolytic oxidation of copper in an aluminate based electrolyte with the respective additives of Na₃PO₄, NaH₂PO₄ and NaH₂PO₂. Applied Surface Science, 565, 150477.
- Greczynski, G., & Hultman, L. (2020). X-ray photoelectron spectroscopy: towards reliable binding energy referencing. *Progress in Materials Science*, 107, 100591.
- Huang, J., Hou, B., Guo, N., Xu, R., Su, N., Bairu, A.G., Huang, X., Xie, C., & Hao, H. (2018). Solid-liquid phase equilibria of ternary system Na₂S₂O₃-Na₂SO₄-H₂O in a wide range of temperatures: measurement and application. *The Journal of Chemical Thermodynamics*, 125, 1-10.
- Huang, X., Wang, G., Huang, M., Deng, Y., Fei, M., Xu, C., & Cheng, J. (2017). Ce³⁺ doped CeP₂O₇ ceramic electrolyte for high temperature proton exchange membrane fuel cell. *International Journal of Electrochemical Science*, *12*(4), 2731-2740.
- Jain, V., Biesinger, M.C., & Linford, M.R. (2018). The Gaussian-Lorentzian sum, product, and convolution (Voigt) functions in the context of peak fitting X-ray photoelectron spectroscopy (XPS) narrow scans. *Applied Surface Science*, 447, 548-553.
- Janoš, P., Henych, J., Pfeifer, J., Zemanová, N., Pilařová, V., Milde, D., & Štengl, V. (2017). Nanocrystalline cerium oxide prepared from a carbonate precursor and its ability to breakdown biologically relevant organophosphates. *Environmental Science: Nano*, 4(6), 1283-1293.



- Jian, S., Tzeng, Y., Ger, M., Chang, K., Shi, G., Huang, W., Chen, C., & Wu, C. (2020). The study of corrosion behavior of manganese-based conversion coating on LZ91 magnesium alloy: effect of addition of pyrophosphate and cerium. *Materials & Design*, 192, 108707.
- Kloprogge, J.T., & Wood, B.J. (2016). Systematic XPS study of gallium-substituted boehmite. *Journal of Materials Science*, *51*, 5436-5444.
- Kumar, P., Parashar, M., Chauhan, K., Chakraborty, N., Sarkar, S., Chandra, A., Das, N.S., Chattopadhyay, K.K., Ghoari, A., Adalder, A., & Banerjee, D. (2023). Significant enhancement in the cold emission characteristics of chemically synthesized super-hydrophobic zinc oxide rods by nickel doping. *Nanoscale Advances*, *5*(24), 6944-6957.
- Kumar, P., Veer, D., Singh, D., & Meena, S.L. (2024). A parametric study of crystal structure, phase stability, and conductivity of the novel phosphate-based composite electrolyte. *Applied Physics A*, 130(4), 249.
- Lubenchenko, A.V., Batrakov, A.A., Pavolotsky, A.B., Lubenchenko, O.I., & Ivanov, D.A. (2018). XPS study of multilayer multicomponent films. *Applied Surface Science*, 427, 711-721.
- Mallet, M., Barthélémy, K., Ruby, C., Renard, A., & Naille, S. (2013). Investigation of phosphate adsorption onto ferrihydrite by X-ray photoelectron spectroscopy. *Journal of Colloid and Interface Science*, 407, 95-101.
- Martsinkevich, V.V., & Ponomareva, V.G. (2012). Double salts Cs1- xM_xH₂PO₄ (M= Na, K, Rb) as proton conductors. *Solid State Ionics*, 225, 236-240.
- Moudler, J.F., Stickle, W.F., Sobol, P.E., & Bomben, K.D. (1992). Handbook of X-ray photoelectron spectroscopy. *Perkin-Elmer, Eden Prairie, MN*, 52.
- Owens, B.B. (2000). Solid state electrolytes: overview of materials and applications during the last third of the Twentieth Century. *Journal of Power Sources*, 90(1), 2-8.
- Rhimi, T., Leroy, G., Duponchel, B., Khirouni, K., Guermazi, S., & Toumi, M. (2018). Electrical conductivity and dielectric analysis of NaH₂PO₄ compound. *Ionics*, 24, 3507-3514.
- Rybalkina, O., Tsygurina, K., Melnikova, E., Mareev, S., Moroz, I., Nikonenko, V., & Pismenskaya, N. (2019). Partial fluxes of phosphoric acid anions through anion-exchange membranes in the course of NaH₂PO₄ solution electrodialysis. *International Journal of Molecular Sciences*, 20(14), 3593.
- Singh, P., Sharma, A.K., & Kumar, P. (2024a). Review of the literature on the thermal stability and conductivity of solid acid fuel cells. *Macromolecular Symposia*, 413(5), 2400119.
- Singh, P., Sharma, A.K., Kumar, P., Veer, D., Kumar, D., Singh, D., & Katiyar, R.S. (2024b). Role of pyrophosphate source for improving proton conductivity and stability of sodium dihydrogen phosphate. *Russian Journal of Inorganic Chemistry*, 1-9. https://doi.org/10.1134/S0036023624601338.
- Siow, K.S., Britcher, L., Kumar, S., & Griesser, H.J. (2018). XPS study of sulfur and phosphorus compounds with different oxidation states. *Sains Malaysiana*, 47(8), 1913-1922.
- Stevie, F.A., & Donley, C.L. (2020). Introduction to x-ray photoelectron spectroscopy. *Journal of Vacuum Science & Technology A*, *38*, 063204. https://doi.org/10.1116/6.0000412.
- Teterin, Y.A., Teterin, A.Y., Lebedev, A.M., & Utkin, I.O. (1998). The XPS spectra of cerium compounds containing oxygen. *Journal of Electron Spectroscopy and Related Phenomena*, 88, 275-279.
- Uma, T., Mahalingam, T., Gaur, M.S., & Sharma, A.K. (2014). Synthesis and characterization of solid SiO₂/P₂O₅/ZrO₂ PVP membrane for fuel cell applications. *International Journal of Membrane Science and Technology*, 1, 31-36.
- Veer, D., Kumar, P., Singh, D., Kumar, D., & Katiyar, R.S. (2022). A synergistic approach to achieving high conduction and stability of CsH₂PO₄/NaH₂ PO₄/ZrO₂ composites for fuel cells. *Materials Advances*, *3*(1), 409-417.



- Yao, J., Sun, H., Ban, X., & Yin, W. (2021). Analysis of selective modification of sodium dihydrogen phosphate on surfaces of magnesite and dolomite: reverse flotation separation, adsorption mechanism, and density functional theory calculations. *Colloids and Surfaces A: Physicochemical and Engineering Aspects*, 618, 126448.
- Yoshimi, S., Matsui, T., Kikuchi, R., & Eguchi, K. (2008). Temperature and humidity dependence of the electrode polarization in intermediate-temperature fuel cells employing CsH₂PO₄/SiP₂O₇-based composite electrolytes. *Journal of Power Sources*, 179(2), 497-503.
- Zhang, L., Liu, Y., Wang, Y., Li, X., & Wang, Y. (2021). Investigation of phosphate removal mechanisms by a lanthanum hydroxide adsorbent using p-XRD, FTIR and XPS. *Applied Surface Science*, 557, 149838.
- Zhang, X., Liu, C., Shen, W., Ren, Y., Li, D., & Yang, H. (2015). Solubility and physic-chemical properties of NaH2PO4 in phosphoric acid, sodium chloride and their mixture solutions at T=(298.15 and 313.15) K. *The Journal of Chemical Thermodynamics*, 90, 185-192.
- Zhang, X., Ren, Y., Ma, W., & Ma, H. (2014). (Solid+ liquid) phase equilibrium for the ternary system (NaCl+ NaH₂PO₄+H₂O) at T=(298.15 and 313.15) K and atmospheric pressure. *The Journal of Chemical Thermodynamics*, 77, 107-111.



Original content of this work is copyright © Ram Arti Publishers. Uses under the Creative Commons Attribution 4.0 International (CC BY 4.0) license at https://creativecommons.org/licenses/by/4.0/

Publisher's Note- Ram Arti Publishers remains neutral regarding jurisdictional claims in published maps and institutional affiliations.